



**HAL**  
open science

## Predictive control of activated sludge plants to supply nitrogen for optimal crop growth

Otacílio B L Neto, Antoine Haddon, Farouk Aichouche, Jérôme Harmand, Michela Mulas, Francesco Corona

### ► To cite this version:

Otacílio B L Neto, Antoine Haddon, Farouk Aichouche, Jérôme Harmand, Michela Mulas, et al.. Predictive control of activated sludge plants to supply nitrogen for optimal crop growth. IFAC-PapersOnLine, 2021, 54 (3), pp.200-205. 10.1016/j.ifacol.2021.08.242 . hal-03361156

**HAL Id: hal-03361156**

**<https://hal.inrae.fr/hal-03361156>**

Submitted on 1 Oct 2021

**HAL** is a multi-disciplinary open access archive for the deposit and dissemination of scientific research documents, whether they are published or not. The documents may come from teaching and research institutions in France or abroad, or from public or private research centers.

L'archive ouverte pluridisciplinaire **HAL**, est destinée au dépôt et à la diffusion de documents scientifiques de niveau recherche, publiés ou non, émanant des établissements d'enseignement et de recherche français ou étrangers, des laboratoires publics ou privés.



Distributed under a Creative Commons Attribution - NonCommercial - NoDerivatives 4.0 International License

## Predictive control of activated sludge plants to supply nitrogen for optimal crop growth

Otacílio B. L. Neto\* Antoine Haddon\*\* Farouk Aichouche\*\*  
Jérôme Harmand\*\* Michela Mulas\* Francesco Corona\*\*\*\*

\* Postgraduate Programme in Teleinformatics Engineering, Federal University of Ceará, Brazil. (e-mails: [minhotmog@alu.ufc.br](mailto:minhotmog@alu.ufc.br), [michela.mulas@ufc.br](mailto:michela.mulas@ufc.br))

\*\* INRAE, Univ Montpellier, LBE, Narbonne, France. (e-mails: {[antoine.haddon](mailto:antoine.haddon), [farouk.aichouche](mailto:farouk.aichouche), [jerome.harmand](mailto:jerome.harmand)}@inrae.fr)

\*\*\* School of Chemical Engineering, Aalto University, Finland. (email: [francesco.corona@aalto.fi](mailto:francesco.corona@aalto.fi))

**Abstract:** We report the preliminary results of a feasibility study in which we investigate the possibility to operate a common class of activated sludge plants to produce effluent wastewater of varying quality for crop irrigation. Firstly, a nitrogen reference trajectory is computed as solution to a higher-level optimal control problem that aims at maximizing plant biomass in a crop growth system. We then study how to control the treatment plant with a zero-offset predictive control strategy designed to operate the treatment process to supply nitrogen according to this optimal planning for crop growth. We show how an *ad hoc* tuning of the predictive controller allows to define alternative policies that favour the manipulation of different forms of nitrogen in the treatment plant. We show that the designed controllers are only partially capable to operate the treatment plant to meet the nitrogen demand, when subjected to typical municipal wastewater influent conditions. However, zero-offset can be achieved under constant influent conditions. We analyse the performance of the controller in terms of tracking accuracy and operational energy.

Copyright © 2021 The Authors. This is an open access article under the CC BY-NC-ND license (<http://creativecommons.org/licenses/by-nc-nd/4.0>)

**Keywords:** Model predictive control, optimal control, activated sludge process, crop growth.

### 1. INTRODUCTION

The sustainable management of water resources is attaining unprecedented importance when trying to address the implications of climate change, raising population, and the public expectations for high service standards. As it alleviates the need for fresh water, wastewater reuse is one of the practices which has proven itself inherently circular and useful in satisfying the supply of water of varying quality for industrial, urban and agricultural activities.

The reclamation of municipal wastewater is especially valuable for crop fertigation, as the same nutrients found in wastewater are also main contributors to plant growth. Specifically, the nitrogen compounds in the soil are known to be key factors for crop development (Pelak et al., 2017). These compounds are also central to activated sludge processes in conventional wastewater treatment plants. While many control strategies for optimising the operation of wastewater treatment plants have been proposed (Olsson et al., 2014), their use for water reclamation is an active research area with important challenges for the health of the public and the environment (Ait Mouheb et al., 2018).

This work investigates the feasibility of operating a wastewater treatment plant to produce a reusable water of

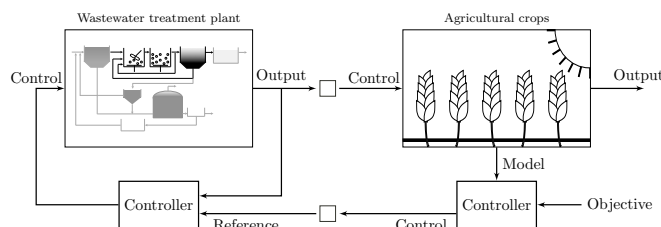


Fig. 1. Control hierarchy of the crop-treatment system.

tailored quality for crop irrigation. We focus on the predictive control of activated sludge plants, as described by the Benchmark Simulation Model no. 1 (BSM1, Gernaey et al. (2014)), and the problem of tracking an effluent of varying nitrogen content. The control problem is approached using a lower-level zero-offset controller on a reference trajectory obtained from solving a higher-level optimal control that maximizes plant biomass within a crop growth system. The coupling between these two systems is depicted in Fig. 1.

According to our results, the controllers are only partially capable to operate the BSM1 to meet the nitrogen demand when subjected to typical influent conditions. However, zero-offset can be achieved under constant influent conditions. We show how the controller favours the manipulation of  $\text{NO}_2^- + \text{NO}_3^-$  or  $\text{NH}_4^+ + \text{NH}_3$  nitrogen, depending on whether the steady-inputs used for linearisations are minimized or let free, respectively. We analyse each controller in terms of tracking accuracy and operational energy.

\* This work has been done within the international project Control4Reuse, part of the IC4WATER programme, in the frame of the collaborative international consortium of the Water Challenges call 2017, Changing World Joint Programme Initiative (Water JPI).

## 2. THE AGRICULTURAL CROP SYSTEM

This section presents the optimal control for maximizing plant biomass using a simplified crop growth model. We overview the state-space model used by the controller, formulate its optimisation task and discuss the results.

### 2.1 State-space model

We consider the model of a crop grown in monoculture that is irrigated continuously with treated wastewater over the course of a growing season on a uniform area of land at field-scale. As a first approach, we assume the idealized model of Pelak et al. (2017) describing a simplified crop development process focused on the water and nitrogen dynamics of the crop and soil. From a system perspective, the dynamics are described using the variables at Table 1.

Table 1. Crop model: State and input variables.

	Description [Units]
$C$	Canopy cover [ $\text{m}^2 \text{m}^{-2}$ ]
$B$	Crop biomass per unit area [ $\text{kg m}^{-2}$ ]
$S$	Relative Soil moisture [ $\text{m}^3 \text{m}^{-3}$ ]
$N$	Nitrogen content per unit area of soil [ $\text{g m}^{-2}$ ]
$I$	Irrigation flow-rate per unit area [ $\text{mm d}^{-1}$ ]
$F_N$	Nitrogen concentration of irrigation water [ $\text{g m}^{-3}$ ]

The state-space model for the crop system is given by

$$\dot{x}_C(t) = f_C(x_C(t), u_C(t)|\theta_C), \quad (1)$$

with state  $x_C = [C \ B \ S \ N]^T \in \mathbb{R}_{\geq 0}^4$  and input  $u_C = [I \ F_N] \in \mathbb{R}_{\geq 0}^2$ . The time-invariant dynamics  $f_C(\cdot|\theta_C)$  depend on a set of parameters (Pelak et al., 2017) denoted by  $\theta_C$ . We consider the parameters referring to the dynamics of a modern corn cultivar grown on a silty loam type soil.

We adapt the model by defining the fertilization term  $F(t) = I(t)F_N(t)$ . As a simplification, we consider the absence of any rainfall and assume constant reference evapotranspiration, the water loss due to the impact of climate on evaporation and plant transpiration.

### 2.2 Optimal control formulation

We consider the problem of maximizing crop biomass at the end of a growing season. This task is formalised by the finite-horizon optimal control problem in the form

$$\max_{u_C(\cdot)} B(T) \quad (2a)$$

$$\text{s.t. } \dot{x}_C(t) = f_C(x_C(t), u_C(t)|\theta_C), \quad (2b)$$

$$\forall t \in [0, T] \quad u_C(t) \in [0, I^{\max}] \times [0, F_N^{\max}], \quad (2c)$$

$$x_C(0) = x_0, \quad (2d)$$

for fixed final time  $T$ , initial state  $x_0$ , and input upper bounds  $I^{\max}$  and  $F_N^{\max}$ . We restrict ourselves to growing seasons lasting  $T = 140\text{d}$ . In the following, we present the optimal control solutions over several simulated scenarios. Each non-linear optimisation Eq. (2) is solved using a dynamic programming approach (Bonnans et al., 2017).

### 2.3 Nitrogen demand for optimal crop growth

We analyse the optimal control results over three different scenarios corresponding to different initial soil nitrogen

content, Fig. 2. We consider the same initial conditions for the remaining state-variables in all scenarios. The initial nitrogen and control results are summarised in Table 2.

Table 2. Scenarios: Initial nitrogen soil conditions and control results.

	$N(0)$	$F_{TOT}$	$N_{TOT}$	$B(T)$
Scenario I	1.00	38.50	39.50	2.44
Scenario II	8.20	23.00	31.20	2.88
Scenario III	15.00	16.20	31.20	2.88

State trajectories show similar behaviour in all cases. The resulting controls focus on maintaining soil water and nitrogen content at the critical levels above which the plant is not under stress. As the model includes water and nitrogen stresses as a reduction of crop growth, it is clearly optimal to maintain the system above such levels.

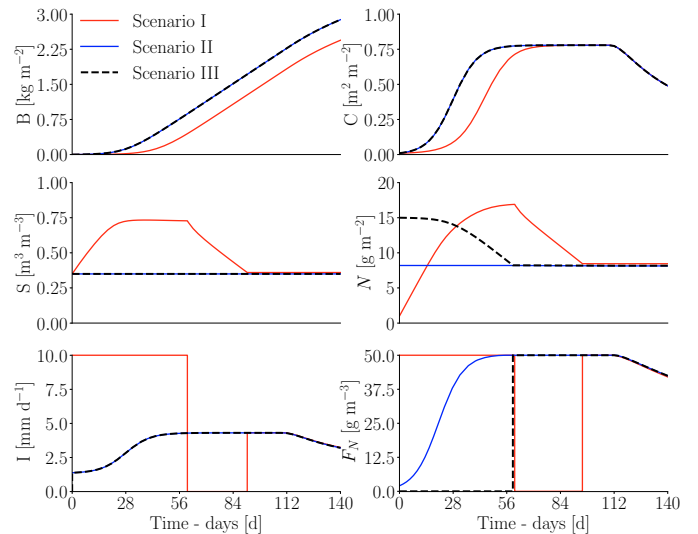


Fig. 2. Crop: Maximimisation of  $B(T)$  for all scenarios.

We summarise and compare each result using the total fertigation  $F_{TOT} = \int_0^T I(t)F_N(t)dt$  and the resulting total nitrogen  $N_{TOT} = N(0) + F_{TOT}$ , Table 2. For Scenario I, the controller must supply more nitrogen to the crop than in Scenarios II and III. However, this does not translate into more biomass as the crop is initially under stress and the controls are unable to drive the soil nitrogen to the critical level fast enough. Conversely, we note that Scenarios II and III achieve the same final biomass  $B(T)$  and also the same total nitrogen  $N_{TOT}$ . This indicates that there is no benefit from supplying nitrogen in excess.

## 3. THE ACTIVATED SLUDGE PLANT

This section presents the predictive controller for supplying nitrogen to a crop growth system (Section 2) using the biological process in a conventional wastewater treatment plant. We overview the state-space model of the activated sludge plant used by the controller and formulate its design as solution to a general trajectory optimisation task.

### 3.1 State-space model

The prototypical activated sludge process in a conventional wastewater treatment plant consists of five biological reactors and a settler, Fig. 3. The treatment starts in a first

reactor where wastewater from primary sedimentation, return sludge from secondary sedimentation and internal recycle sludge are fed. Mixed liquor from the fifth reactor is recirculated into the first reactor together with the recycle sludge from secondary sedimentation, as mentioned. Oxygen can be added by insufflating air into each reactor. In the aerated reactors, ammonium nitrogen contained in the wastewater is oxidised into nitrate nitrogen, which is in turn reduced into nitrogen gas in the anoxic reactors. Extra carbon can be added to each tank independently.

Each reactor is described by the Activated Sludge Model no. 1, while the settler is described by a 10-layer non-reactive model. This process corresponds to the Benchmark Simulation Model no. 1 (Gernaey et al., 2014) and it will be referred to as the activated sludge plant (ASP).

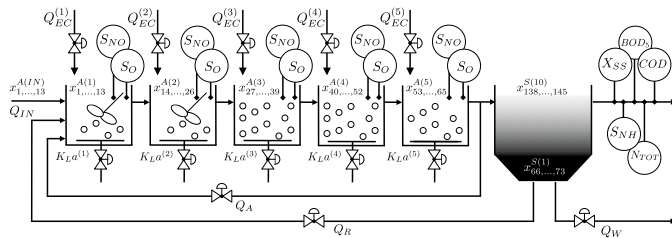


Fig. 3. The activated sludge plant: Process layout.

From the system perspective, the dynamics of each reactor  $A^{(r)}$  ( $r = 1, \dots, 5$ ), if studied individually, are described by using 13 state variables, the vector of concentrations

$$x^{A(r)} = [S_I^{A(r)} \ S_S^{A(r)} \ X_I^{A(r)} \ X_S^{A(r)} \ X_{BH}^{A(r)} \ X_{BA}^{A(r)} \\ X_P^{A(r)} \ S_O^{A(r)} \ S_{NO}^{A(r)} \ S_{NH}^{A(r)} \ S_{ND}^{A(r)} \ X_{ND}^{A(r)} \ S_{ALK}^{A(r)}]^\top,$$

and two controllable inputs,  $u^{A(r)} = [K_L a^{(r)} \ Q_{EC}^{(r)}]$ , the oxygen transfer coefficient  $K_L a^{(r)}$  and the external carbon source flow-rate  $Q_{EC}^{(r)}$ . The dynamics of each settler's layer  $S^{(l)}$  ( $l = 1, \dots, 10$ ) are individually described by using 8 state variables, the vector of concentrations

$$x^{S(l)} = [X_{SS}^{S(l)} \ S_I^{S(l)} \ S_S^{S(l)} \ S_O^{S(l)} \ S_{NO}^{S(l)} \ S_{NH}^{S(l)} \ S_{ND}^{S(l)} \ S_{ALK}^{S(l)}]^\top.$$

The activated sludge plant is subjected to three additional controllable inputs, the internal and external sludge recycle flow-rates ( $Q_A$  and  $Q_R$ , respectively) and the wastage flow-rate  $Q_W$ , and to 14 disturbances, the influent flow-rate  $Q_{IN}$  and its concentrations  $x^{A(IN)}$ , all directly entering the first reactor. Wastewater concentrations for the internal recycle are given by  $x^{A(5)}$ , whereas  $x^{S(1)}$  are the concentrations in the external recycle and wastage flow.

As for the measurements, we consider a typical sensor-arrangement in which we assume the existence of a set of analysers determining, online, the vector of concentrations

$$y = [S_O^{A(1)} \ \dots \ S_O^{A(5)} \ S_{NO}^{A(1)} \ \dots \ S_{NO}^{A(5)} \ X_{SS}^{S(10)} \\ S_{NH}^{S(10)} \ BOD_5^{S(10)} \ COD^{S(10)} \ N_{TOT}^{S(10)}]^\top.$$

The composite variables, biochemical oxygen demand ( $BOD_5$ ), chemical oxygen demand ( $COD$ ), total nitrogen ( $N_{TOT}$ ) and total suspended solids ( $X_{SS}$ ), are computed as in Gernaey et al. (2014). Specifically,  $N_{TOT}$  is given by

$$N_{TOT} = S_{NO} + S_{NH} + S_{ND} + X_{ND} \\ + i_{XB}(X_{BH} + X_{BA}) + i_{XP}(X_P + X_I),$$

with stoichiometric parameters ( $i_{XB}$ , and  $i_{XP}$ ).

The state-space model for this class of bioprocesses is thus,

$$\dot{x}(t) = f(x(t), u(t), w(t)|\theta_x); \quad (3a)$$

$$y(t) = g(x(t)|\theta_y), \quad (3b)$$

with state  $x(t) = [x^{A(1)} \ \dots \ x^{A(5)} \ x^{S(1)} \ \dots \ x^{S(10)}]^\top \in \mathbb{R}_{\geq 0}^{N_x}$ , measurements  $y(t) \in \mathbb{R}_{\geq 0}^{N_y}$ , controllable input  $u(t) = [Q_A \ Q_R \ Q_W \ u^{A(1)} \ \dots \ u^{A(5)}]^\top \in \mathbb{R}_{\geq 0}^{N_u}$ , and uncontrollable input  $w(t) = [Q_{IN} \ x^{A(IN)}]^\top \in \mathbb{R}_{\geq 0}^{N_w}$ . The time-invariant dynamics  $f(\cdot|\theta_x)$  and  $g(\cdot|\theta_y)$  depend on a set of stoichiometric and kinetic parameters (Gernaey et al., 2014) collectively denoted by the vectors  $\theta_x$  and  $\theta_y$ . The model in Eq. (3) thus consists of  $N_x = 13 \times 5 + 8 \times 10 = 145$  state variables,  $N_u = 3 + 5 \times 2 = 13$  controllable inputs,  $N_w = 1 + 13 = 14$  disturbances and  $N_y = 15$  outputs. The described state-space configuration includes all the control handles in Gernaey et al. (2014) that do not require changes to the plant layout. We also refer to Gernaey et al. (2014) for a detailed description of the process variables.

The influent conditions used in the experiments correspond to the long-term scenario provided by the benchmark. The data consists of flow-rate and composition of wastewater from primary sedimentation sampled every 15 minutes over a period of 609 days. The sample for  $t = 0.625d$  is used as initial condition for all simulations.

### 3.2 Predictive controller

We formulate the trajectory optimisation task as an on-line optimal control problem and we consider a discretise-then-optimise approach to the design of the predictive controller. We approximate the desired output trajectory with a sequence of piecewise-constant set-points and, at each discretisation point in time, we linearise the model about an optimally selected fixed-point that satisfy the trajectory. The sequence of zero-offset controls are then computed by solving the resulting regulation constrained by the linearised dynamics and state and input bounds.

*Model discretisation and linearisation* For each time interval  $t \in [t_k, t_{k+1})$ , we consider piecewise constant inputs  $u(t) = u(t_k)$  and  $w(t) = w(t_k)$  with  $t_k = k\Delta t$  the  $k$ -th time instant given period  $\Delta t > 0$ . The discrete-time dynamics are given by the transition function

$$x_{k+1} = f_{\Delta t}(x_k, u_k, w_k|\theta_x) = x_k + \int_0^{\Delta t} f(x(\tau), u_k, w_k|\theta_x) d\tau,$$

with  $x_k = x(k\Delta t)$ ,  $u_k = u(k\Delta t)$ , and  $w_k = w(k\Delta t)$ . The discrete-time output equation is  $y_k = y(k\Delta t) = g(x_k|\theta_y)$ . In general, the transition function is solved numerically, but it can be solved analytically when  $f(\cdot|\theta_x)$  is linear.

The nonlinear dynamics (and measurement process) in the vicinity of any point  $P \equiv (\tilde{x}, \tilde{u}, \tilde{w}, \tilde{y})$  can be linearised as

$$\dot{\delta x}(t) = z_f + A\delta x(t) + B\delta u(t) + G\delta w(t); \quad (4a)$$

$$y(t) = z_g + C\delta x(t), \quad (4b)$$

with Jacobian matrices  $A = (\partial f/\partial x)|_P \in \mathbb{R}^{N_x \times N_x}$ ,  $B = (\partial f/\partial u)|_P \in \mathbb{R}^{N_x \times N_u}$ ,  $G = (\partial f/\partial w)|_P \in \mathbb{R}^{N_x \times N_w}$  and  $C = (\partial g/\partial x)|_P \in \mathbb{R}^{N_y \times N_x}$ , and constant vectors  $z_f = f(\tilde{x}, \tilde{u}, \tilde{w}|\theta_x)$  and  $z_g = g(\tilde{x}|\theta_y)$ , evaluated at such point. The variable  $\delta x(t) = x(t) - \tilde{x}$  (respectively,  $\delta u(t) = u(t) - \tilde{u}$  and  $\delta w(t) = w(t) - \tilde{w}$ ), refers to the state (inputs and disturbances) deviation from the linearisation point.

The analytical solution of the transition function  $f_{\Delta t}(\cdot|\theta_x)$  given Eq. (4) leads to the discrete-time state-space

$$x_{k+1} = z_{f_{\Delta t}} + A_{\Delta t}\delta x_k + B_{\Delta t}\delta u_k + G_{\Delta t}\delta w_k; \quad (5a)$$

$$y_k = z_g + C\delta x_k, \quad (5b)$$

with  $A_{\Delta t} = e^{A\Delta t}$ ,  $B_{\Delta t} = S_{\Delta t}B$ ,  $G_{\Delta t} = S_{\Delta t}G$ , and vector  $z_{f_{\Delta t}} = S_{\Delta t}z_f$ , given  $S_{\Delta t} = A^{-1}(e^{A\Delta t} - I)$ . The discrete-time counterpart of the deviation variables are given by  $\delta x_k = x_k - \tilde{x}$ ,  $\delta u_k = u_k - \tilde{u}$  and  $\delta w_k = w_k - \tilde{w}$ .

*Trajectory linearisation* For a reference output  $\tilde{y}^{sp}(t) \in \mathbb{R}^{N_{\tilde{y}}}$  and input  $u^{sp}(t) \in \mathbb{R}^{N_u}$ , the optimal linearisation point  $P^{(k)} = (\tilde{x}_k, \tilde{u}_k, \tilde{w}_k, \tilde{y}_k)$  is the pair  $(\tilde{x}_k, \tilde{u}_k)$  that solves

$$\min_{\tilde{x}_k, \tilde{u}_k} \|Hg(\tilde{x}_k) - \tilde{y}_k^{sp}\|_{W_y}^2 + \|\tilde{u}_k - u_k^{sp}\|_{W_u}^2 \quad (6a)$$

$$\text{s.t. } f(\tilde{x}_k, \tilde{u}_k, \tilde{w}_k|\theta_x) = 0, \quad (6b)$$

$$\tilde{x}_k \in \mathcal{X}^{sp}, \quad \tilde{u}_k \in \mathcal{U}^{sp}. \quad (6c)$$

with  $\tilde{y}_k^{sp} = \tilde{y}^{sp}(\lfloor \frac{k\Delta t}{\Delta t_{sp}} \rfloor \Delta t_{sp})$  and  $u_k^{sp} = u^{sp}(\lfloor \frac{k\Delta t}{\Delta t_{sp}} \rfloor \Delta t_{sp})$  the set-points over the sampling period  $\Delta t_{sp} > 0$ , and known disturbance  $\tilde{w}_k$ . Matrix  $H \in \{0, 1\}^{N_{\tilde{y}} \times N_y}$  selects the  $N_{\tilde{y}} \leq N_y$  outputs of interest.  $(A^{(k)}, B^{(k)}, G^{(k)}, C^{(k)})$  is used to denote the model linearised around  $P^{(k)}$ , Eq. (4).

In Eq. (6), we assume symmetric weighting matrices  $W_y, W_u \succeq 0$ . Input references are set constant  $u^{sp}(t) = 0$ . The steady-state  $\tilde{x}_k$  is constrained to be non-negative ( $\mathcal{X}^{sp} = \mathbb{R}_{\geq 0}^{N_x}$ ) and the set  $\mathcal{U}^{sp} \subseteq \mathbb{R}^{N_u}$  is defined by actuators bounds. The disturbances  $\tilde{w}_k = \tilde{w}$  for linearisation are the average influent conditions in Gerney et al. (2014).

*Optimal control* At each instant  $k \in \mathbb{N}$ , we first solve the finite-horizon optimal control problem in the general form

$$\min_{u_k, \dots, u_{k+N-1}} \sum_{n=k}^{k+N-1} L(x_n, u_n) + L_f(x_{k+N}) \quad (7a)$$

$$\text{s.t. } x_{n+1} = f_{\Delta t}(x_n, u_n, w_n|\theta_x), \quad (7b)$$

$$\forall n \in [k, k+N] \quad x_n \in \mathcal{X}, \quad u_n \in \mathcal{U}, \quad (7c)$$

$$\Phi(x_k, x_{k+N}) = 0, \quad (7d)$$

and then we apply the first control action to the process.

We consider state regulation problems with quadratic cost functions  $L(x, u) = \|x - \tilde{x}_k\|_Q^2 + \|u - \tilde{u}_k\|_R^2$ , for symmetric matrices  $Q \succeq 0$  and  $R \succ 0$ , and steady-state  $\tilde{x}_k \in \mathbb{R}^{N_x}$  and steady-input  $\tilde{u}_k \in \mathbb{R}^{N_u}$ . The terminal cost is defined as  $L_f(x) = L(x, 0)$ . The dynamics  $f_{\Delta t}(\cdot|\theta_x)$  with outputs  $g(\cdot|\theta_y)$  are represented by the discrete-time state-space, Eq. (5), for linearisation  $(A^{(k)}, B^{(k)}, G^{(k)}, C^{(k)})$ . State trajectories are assumed to be implicitly constrained by the model dynamics, or unconstrained ( $\mathcal{X} = \mathbb{R}^{N_x}$ ). Constraint set  $\mathcal{U} \subseteq \mathbb{R}^{N_u}$  is defined by the set of linear inequalities corresponding to the actuators bounds. We assume only initial constraint  $\Phi(x_k, x_{k+N}) = x_k - \hat{x}_k$  given initial state  $\hat{x}_k$  directly measured from the plant. Finally, disturbances are held constant over each horizon,  $w_n = \hat{w}_k$  ( $n = k, \dots, k+N$ ), with  $\hat{w}_k$  known. To satisfy a realistic setup, disturbances are assumed to be measured given a sampling period  $\Delta t_w > 0$  such that  $\hat{w}_k = w(\lfloor \frac{k\Delta t}{\Delta t_w} \rfloor \Delta t_w)$ .

We solve each optimisation (Eq. 7) by the direct method of transcribing the problem into a standard nonlinear program, then casted as a convex quadratic program with linear constraints and solved numerically (Betts, 2010).

## 4. RESULTS AND DISCUSSION

In this section, we present the simulation results obtained by the predictive control of the activated sludge plant (Section 3) when the process is requested to produce nitrogen for optimal crop growth (Section 2). We illustrate the results with two tuning configurations of the controller, one favouring the manipulation of  $\text{NO}_2^- + \text{NO}_3^-$  nitrogen ( $S_{NO}$ ) and another one favouring  $\text{NH}_4^+ + \text{NH}_3$  nitrogen ( $S_{NH}$ ). We first present the configuration settings that are common to both controllers, then we discuss the specific parameters and results separately. The performances are evaluated under constant and dynamic disturbance regimes in terms of tracking accuracy and operation energy consumption.

We consider reference trajectories for total nitrogen  $N_{TOT}^{S(10)}$  in the effluent that corresponds to the nitrogen concentration of irrigation water,  $\tilde{y}^{sp}(t) = F_N^*(t)$ . This corresponds to  $H = [0 \ \dots \ 1]$  in Eq. (6). The sampling period of the reference is  $\Delta t_{sp} = 7\text{d}$ . For the activated sludge plant in Eq. (3), the linear models  $(A^{(k)}, B^{(k)}, G^{(k)}, C^{(k)})$  around  $P^{(k)} \equiv (\tilde{x}_k, \tilde{u}_k, \tilde{w}_k, \tilde{y}_k)$  are computed by solving the optimisation in Eq. (6) once a week, when set-points  $\tilde{y}_k^{sp} = \tilde{y}^{sp}(\lfloor \frac{k\Delta t}{\Delta t_{sp}} \rfloor \Delta t_{sp})$  are available. The dynamics  $f_{\Delta t}(\cdot|\theta_x)$  in Eq. (5a) are evaluated from  $(A^{(k)}, B^{(k)}, G^{(k)}, C^{(k)})$  with a sampling period  $\Delta t = (1/3)\text{d}$ . The control horizon, Eq. (7), is set to be 7 days, or  $N = 21$ . We assume weighting matrices  $Q = C^{(k)\top}C^{(k)}$  and  $R = \text{diag}[10^{-2}I_8 \ 10^4I_5]$ . The influent conditions are assumed to be measured once every  $\Delta t_w = 1\text{d}$ . Initial state  $x(0) = \tilde{x}$  is the steady-state by Gerney et al. (2014). We treat set-points  $y^{sp}(t) = 0$  as corresponding to interrupted irrigation and control the plant for conventional treatment with  $y_k^{sp} = Hg(\tilde{x})$  whenever  $y_k^{sp} = 0$ . This configuration is common to all cases, under both dynamic and constant disturbances. For the latter, the disturbances are  $w(t) = \tilde{w}$ . For brevity, we restrict the discussion of our results only to Scenario I.

### 4.1 Case I: $N_{TOT}$ control favouring $\text{NO}_2^- + \text{NO}_3^-$ nitrogen

To design a controller that favours the production of  $\text{NO}_2^- + \text{NO}_3^-$  nitrogen when asked to track  $\tilde{y}^{sp}(t) = F_N^*(t)$ , we set the steady-state optimisation parameters  $W_y = 100$  and  $W_u = 0$ . The results (Fig. 4) show that the controller is capable to drive the plant towards the reference values under constant influent conditions. However, performances deteriorate when the plant is subject to dynamic influent conditions. This happens when the plant is asked  $y_k^{sp} \geq 40$  g N  $\text{m}^{-3}$ , a target which appears to be an unreachable.

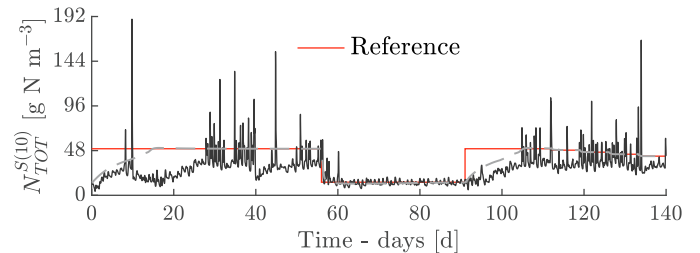


Fig. 4. Case I: Tracking of  $N_{TOT}^{S(10)}$ . Solid/dashed lines refer to solutions under dynamic/constant disturbances.

Figure 5 and 6 depict the control actions and a selection of responses when the controller serves the set-point changes at  $t = \{56, 91\}$ d in Scenario I: The concentration changes are from  $50 \text{ g m}^{-3}$  to  $14.05 \text{ g m}^{-3}$  and back to  $50 \text{ g m}^{-3}$ .

- In the first set-point change  $t = 56$ d, the controller decreases  $N_{TOT}^{S(10)}$  mainly by producing  $S_{NO}^{S(10)}$  nitrogen by explicitly acting on the denitrification-nitrification process: This solution is achieved by first reducing aeration in the first reactors  $A^{(1,2)}$  through  $K_L a^{(1,2)}$ , then, as the concentrations  $S_{NO}^{A(1,2)}$  decrease noticeably, these concentrations are increased in the

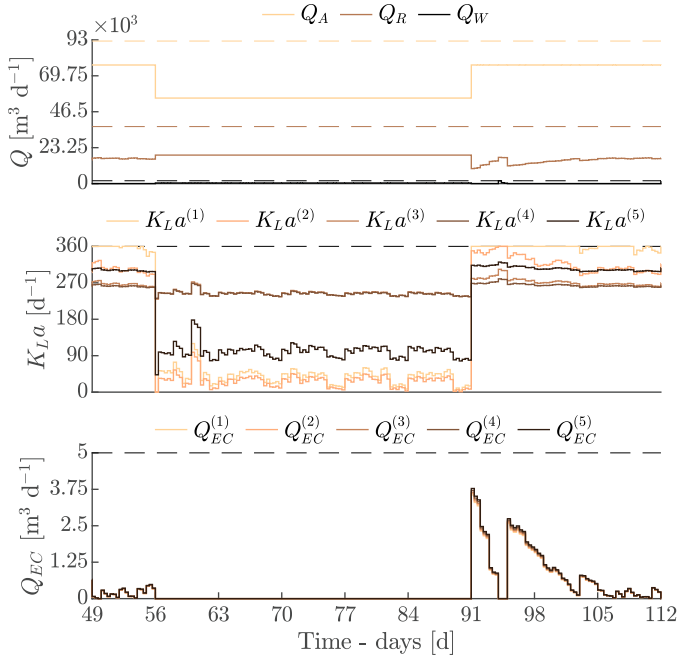


Fig. 5. Case I,  $t \in [49, 112]$ : Flowrates ( $Q_A, Q_R, Q_W$ ), oxygen coefficients  $K_L a^{(1\sim 5)}$ , and extra carbon  $Q_{EC}^{(1\sim 5)}$ .

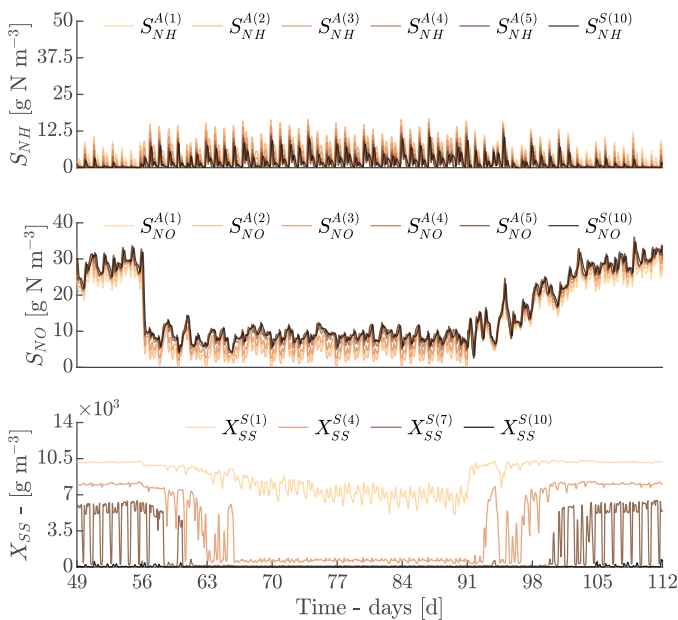


Fig. 6. Case I,  $t \in [49, 112]$ : Nitrogen ( $S_{NH}^{A(1\sim 5)}, S_{NH}^{S(10)}$ ) and ( $S_{NO}^{A(1\sim 5)}, S_{NO}^{S(10)}$ ), and suspended solids  $X_{SS}^{S(1\sim 10)}$ .

last reactors  $A^{(3,4,5)}$  by increasing aeration, through  $K_L a^{(3\sim 5)}$ . Moreover, wastage flow-rate  $Q_W$  is increased to reduce the accumulation of suspended solids  $X_{SS}^{S(1\sim 10)}$  throughout the settler.

- In the second set-point change ( $t = 91$ d), dissolved oxygen is added to all reactors  $A^{(1\sim 5)}$  by increasing  $K_L a^{(1\sim 5)}$ . As a result, nitrification is implemented throughout the entire process. Again, this effect is reflected at concentrations  $S_{NO}^{S(1\sim 10)}$ . As oxygen saturates, however, not enough nitrogen can be converted to reach the set-point. The controller thus attempts to complement the effluent total nitrogen using the nitrogen entrapped in particulate matter. Wastage flow-rate  $Q_W$  is decreased in such way that suspended solids  $X_{SS}^{S(1\sim 10)}$  accumulates in all the settler layers  $S^{(1\sim 10)}$ . Thus,  $N_{TOT}^{S(10)}$  increases due to nitrogen taken from effluent concentrations of biomass ( $X_{BH}^{S(10)}, X_{BA}^{S(10)}$ ) and organic matter ( $X_I^{S(10)}, X_P^{S(10)}$ ).

#### 4.2 Case II: $N_{TOT}$ control favouring $\text{NH}_4^+ + \text{NH}_3$ nitrogen

To favour  $\text{NH}_4^+ + \text{NH}_3$  nitrogen when asked to track  $\hat{y}^{sp}(t) = F_N^*(t)$ , we consider a controller that is based on linearisations ( $A^{(k)}, B^{(k)}, G^{(k)}, C^{(k)}$ ) around points  $P^{(k)} \equiv (\hat{x}_k, \hat{u}_k, \hat{w}_k, \hat{y}_k)$  that solve problem Eq. (6) with weighting matrices configured to be  $W_y = 100$  and  $W_u = 0.01I_{N_u}$ .

The results, Fig. 7, show that also this controller can drive the plant towards the set-points, when operated against constant influent conditions. More importantly, the performance with dynamic influent conditions is improved. For brevity, we report only a selection of responses (Fig. 8) specific to the set-point changes at  $t = \{56, 91\}$ d.

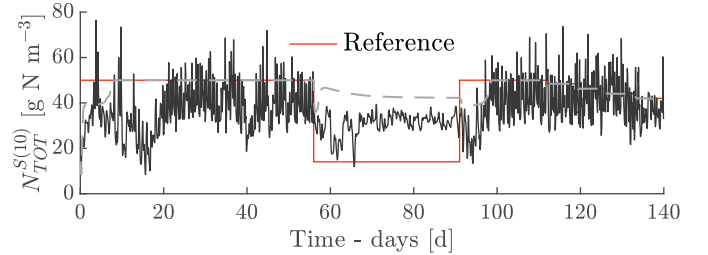


Fig. 7. Case II: Tracking of  $N_{TOT}^{S(10)}$ . Solid/dashed lines refer to solutions under dynamic/constant disturbances.

- In the first change ( $t = 56$ d), the controller attempts to decrease the effluent  $N_{TOT}$  mostly by converting nitrogen from  $S_{NH}$  back to  $S_{NO}$  through nitrification. As the concentrations of  $S_{NO}^{A(1\sim 5)}$  are virtually reduced to zero during the initial interval, not enough nitrogen can be converted in time to reach the set-point. Moreover, wastage flow-rate,  $Q_W$ , is still increased over same interval to reduce the total suspended solids,  $X_{SS}^{S(l)}$ , accumulated in the settler.
- In the second change ( $t = 91$ d), dissolved oxygen is reduced in all reactors by reducing aeration with  $K_L a^{(r)}$ . Again, this is reflected in the ammonia concentrations. As the influent  $\text{NH}_4^+ + \text{NH}_3$  nitrogen is insufficient to reach the set-point, the controller attempts to complement the remaining total nitrogen using nitrogen entrapped in particulate matter.

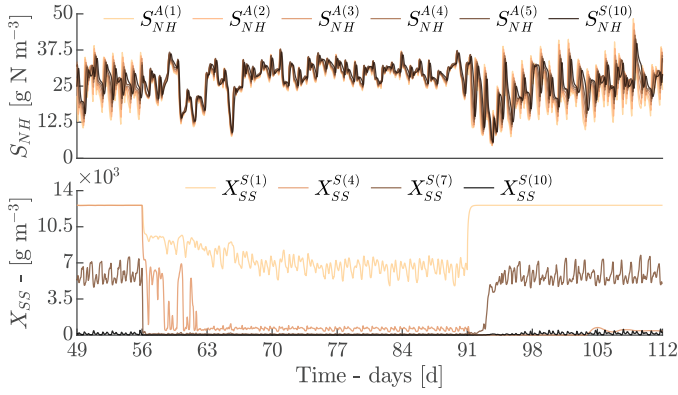


Fig. 8. Case II,  $t \in [49, 112]$ : Nitrogen ( $S_{NH}^{A(1\sim 5)}, S_{NH}^{S(10)}$ ) and solids  $X_{SS}^{S(1\sim 10)}$ .  $S_{NO}^{A(1\sim 5)} = S_{NO}^{S(10)} = 0$ , omitted.

#### 4.3 Case I and Case II: Comparison

We first discuss how disturbances affect the control with respect to Scenario I. We condense the disturbances as influent total nitrogen,  $N_{TOT}^{IN}$ , in Fig. 9 and summarise their effects in terms of nitrogen removal efficiency,  $\eta_{N_{TOT}}(t)$ .

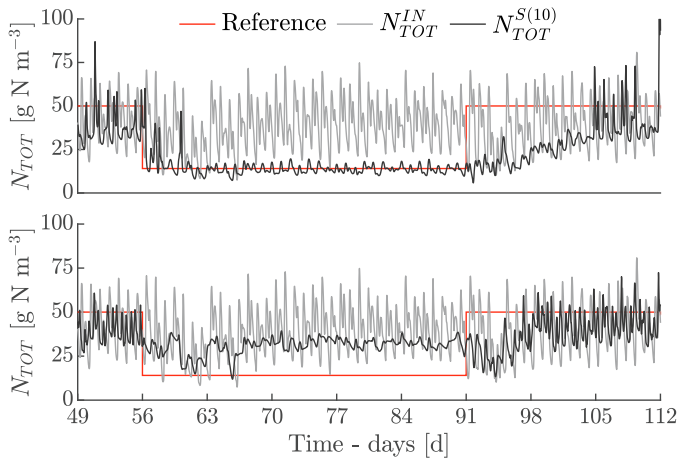


Fig. 9. Comparison,  $t \in [49, 112]$ : Influent and effluent  $N$ .

- Case I: The average  $\overline{\eta_{N_{TOT}}}(t) = 0.57$  indicates that 57% of influent nitrogen is removed in  $t \in [56, 91]$ . Conversely,  $\overline{\eta_{N_{TOT}}}(t) = 0.01$  for  $t \in [49, 56]$  shows that roughly 99% of the influent total nitrogen is still preserved in the effluent during this interval.  $\overline{\eta_{N_{TOT}}}(t) = 0.42$  for  $t \in (91, 112]$  indicates that 58% of influent total nitrogen is still preserved in the effluent.
- Case II: The average  $\overline{\eta_{N_{TOT}}} = 0.10$  for  $t \in [56, 91]$  indicates that only 10% of the influent nitrogen is removed during this time interval. Conversely, average  $\overline{\eta_{N_{TOT}}} = 0.01$  for  $t \in [49, 56] \cup (91, 112]$  indicates that roughly 99% of influent total nitrogen is still preserved in the effluent during this interval.

We evaluate the controllers overall performance by the root mean squared error (RMSE) metric  $J_{RMSE}(y, y^{sp}) = (\frac{1}{140} \int_0^{140} (y(t) - y^{sp}(t))^2 dt)^{1/2}$ . Table 3 shows a general good performance for the control simulations under constant influent conditions. We note that Scenario I with control favouring  $S_{NH}$  (Case II) as an exception, being it unable to reach the set-point for  $t \in [56, 91]$ . Moreover,

results show that performance worsens with dynamic disturbances, being Case II controllers generally less affected.

Table 3.  $J_{RMSE}$ : Tracking accuracy.

		$w(t)$ constant	$w(t)$ dynamic
Case I	Scenario I	8.458	19.720
	Scenario II	3.405	17.989
	Scenario III	5.973	16.372
Case II	Scenario I	15.072	15.743
	Scenario II	1.410	12.899
	Scenario III	3.177	11.068

Finally, we evaluate the overall cost index,  $OCI$ , in (Germaey et al., 2014) considering only the terms for pumping and aeration energy,  $PE$  and  $AE$ , and external carbon,  $EC$ , with a weighting factor  $f_{EC}$ . As expected, Table 4 shows that a solution favouring nitrogen in the form of  $S_{NH}$  costs significantly less than favouring  $S_{NO}$ . Despite the pumping costs being generally low, aeration and carbon addition costs are significantly smaller in Case II.

Table 4. Overall costs comparison [ $\times 10^4$ ].

		$PE$	$AE$	$f_{EC} \cdot EC$	$OCI$
Case I	Scenario I	4.040	14.754	29.911	48.706
	Scenario II	4.239	15.535	25.757	45.531
	Scenario III	3.985	13.472	21.104	38.561
Case II	Scenario I	0.943	2.350	19.123	22.417
	Scenario II	0.442	1.465	11.837	13.745
	Scenario III	1.491	3.360	24.656	29.507

#### REFERENCES

Ait Mouheb, N., Bourrié, G., Thayer, B.B., Benyahia, B., Cherki, B., Condom, N., Declercq, R., Héran, M., Khalifa, R., Molle, B., Patureau, D., Renault, P., Romagny, B., Sinfort, C., Steyer, J.P., Sari, T., Wery, N., and Harmand, J. (2018). The reuse of reclaimed water for irrigation around the mediterranean rim: a step towards a more virtuous cycle? *Regional Environmental Change*, 18(3), 693–705.

Betts, J.T. (2010). *Practical methods for optimal control and estimation using nonlinear programming*. Society for Industrial and Applied Mathematics, 2 edition.

Bonnans, Frederic, J., Giorgi, D., Grelard, V., Heymann, B., Maindrault, S., Martinon, P., Tissot, O., and Liu, J. (2017). Bocop – A collection of examples. Technical report, INRIA. URL <http://www.bocop.org>.

Germaey, K.V., Jeppsson, U., Vanrolleghem, P.A., and Copp, J.B. (2014). *Benchmarking of Control Strategies for Wastewater Treatment Plants*. IWA Publishing.

Olsson, G., Carlsson, B., Comas, J., Copp, J., Germaey, K., Ingildsen, P., Jeppsson, U., Kim, C., Rieger, L., Rodríguez-Roda, I., Steyer, J., Takács, I., Vanrolleghem, P., Vargas, A., Yuan, Z., and Åmand, L. (2014). Instrumentation, control and automation in wastewater - from London 1973 to Narbonne 2013. *Water Science and Technology*, 69(7), 1372–1385.

Pelak, N., Revelli, R., and Porporato, A. (2017). A dynamical systems framework for crop models: Toward optimal fertilization and irrigation strategies under climatic variability. *Ecological Modelling*, 365, 80 – 92.